EBioMedicine 63 (2021) 103206

Contents lists available at ScienceDirect

EBioMedicine

journal homepage: www.elsevier.com/locate/ebiom

Research paper

Recombinant antibody against *Trypanosoma cruzi* from patients with chronic Chagas heart disease recognizes mammalian nervous system.

Leticia L. Niborski[a,1], Mariana Potenza[a], Renato G.S. Chirivi[b,#], Leandro Simonetti[c,#], Micaela S. Ossowski[a,#], Vanina Grippo[a,2], Maria May[d], Daniela I. Staquicini[e,3], Adriana Parodi-Talice[f,g], Carlos Robello[f,h], Marcelo A. Comini[i], Guillermo D. Alonso[a], Jos M.H. Raats[b], Karina A. Gómez[a,*]

[a] *Instituto de Investigaciones en Ingeniería Genética y Biología Molecular (INGEBI-CONICET), Buenos Aires, Argentina*
[b] *ModiQuest B.V., Oss, Netherlands*
[c] *Department of Chemistry – BMC, Uppsala University, Sweden*
[d] *Instituto de Biología y Medicina Experimental (IBYME-CONICET), Buenos Aires, Argentina*
[e] *Departamento de Microbiología, Inmunología e Parasitología, Escola Paulista de Medicina, Universidade Federal de São Paulo, São Paulo, SP, Brazil*
[f] *Unidad de Biología Molecular, Institut Pasteur de Montevideo, Montevideo, Uruguay*
[g] *Sección Genética, Facultad de Ciencias, Universidad de la República, Montevideo, Uruguay*
[h] *Departamento de Bioquímica, Facultad de Medicina, Universidad de la República, Montevideo, Uruguay*
[i] *Group Redox Biology of Trypanosomes, Institut Pasteur de Montevideo, Montevideo, Uruguay*

ARTICLE INFO

Article History:
Received 8 September 2020
Revised 15 October 2020
Accepted 26 November 2020
Available online xxx

Keywords:
Chagas disease
Phage-display
Tubulin
Molecular mimicry
Post-translational modification
Digestive system

ABSTRACT

Background: To deeply understand the role of antibodies in the context of *Trypanosoma cruzi* infection, we decided to characterize A2R1, a parasite antibody selected from single-chain variable fragment (scFv) phage display libraries constructed from B cells of chronic Chagas heart disease patients.
Methods: Immunoblot, ELISA, cytometry, immunofluorescence and immunohistochemical assays were used to characterize A2R1 reactivity. To identify the antibody target, we performed an immunoprecipitation and two-dimensional electrophoresis coupled to mass spectrometry and confirmed A2R1 specific interaction by producing the antigen in different expression systems. Based on these data, we carried out a comparative *in silico* analysis of the protein target's orthologues, focusing mainly on post-translational modifications.
Findings: A2R1 recognizes a parasite protein of ~50 kDa present in all life cycle stages of *T. cruzi*, as well as in other members of the kinetoplastid family, showing a defined immunofluorescence labeling pattern consistent with the cytoskeleton. A2R1 binds to tubulin, but this interaction relies on its post-translational modifications. Interestingly, this antibody also targets mammalian tubulin only present in brain, staining in and around cell bodies of the human peripheral and central nervous system.
Interpretation: Our findings demonstrate for the first time the existence of a human antibody against *T. cruzi* tubulin capable of cross-reacting with a human neural protein. This work re-emphasizes the role of molecular mimicry between host and parasitic antigens in the development of pathological manifestations of *T. cruzi* infection.

1. Introduction

Chagas disease is caused by the parasite *Trypanosoma cruzi* and mainly transmitted to animals and people through contact with feces/urine of vector insects (triatomine or "kissing" bugs). For centuries, Chagas disease was restricted to Central and South America, where it is considered endemic. However, it has now spread to Europe, the United States, Canada, Japan and Australia, due to human migration [1–3]. Chagas disease has two phases: acute and chronic which can be asymptomatic in the majority of infected people (~70%) or it can manifest itself as serious cardiac, digestive, neurological or

* Corresponding author.
E-mail address: gomez@dna.uba.ar (K.A. Gómez).
[1] Present address: Leticia L. Niborski, Institut Curie, PSL Research University, INSERM U932, TransImm Team, Paris, France.
[#] These authors contributed equally to the study.
[2] Present address: Vanina Grippo, Centro de Virología Animal (CEVAN), ICT Milstein-CONICET, Buenos Aires, Argentina.
[3] Present address: Daniela I. Staquicini, Rutgers Cancer Institute of New Jersey, Newark, NJ, USA and Division of Cancer Biology, Department of Radiation Oncology, Rutgers New Jersey Medical School, Newark, NJ, USA.

https://doi.org/10.1016/j.ebiom.2020.103206

Research in context

Evidence before this study

Chagas disease, caused by the parasite *Trypanosoma cruzi*, is linked to poverty and social exclusion. It is endemic in Latin America but is also spreading throughout the world due to population movements. If not treated early after infection, this disease progresses to a chronic form in which some patients develop cardiac or digestive alterations, while others stay asymptomatic. Nowadays, parasite persistence associated with tissue inflammation and cross-reactivity between parasite and host molecules are the two main, non-mutually exclusive mechanisms proposed as an explanation of chronic pathogenesis.

Added value of this study

In this work, we demonstrated that a human monoclonal antibody isolated from B cells of chronic Chagas Disease patients binds to *T. cruzi* tubulin and cross-reacts with a ~50 kDa protein only present in mammalian neural tissue. Interestingly, the antibody binding site on tubulin contains one of the post-translational modifications present in trypanosomatids, and this could be the explanation why the antibody specifically interacts with its neuronal isotype.

Implications of all the available evidence

Our findings raise questions about the pathophysiological role of autoreactive antibodies in chronic Chagas disease.

mixed disorders in up to 30% of cases [3,4]. The interplay between the parasite and the immune response developed by the mammalian host, has a key role in the subsequent clinical outcome of the infection [5,6]. In this regard, antibodies are one of the central components of the host's immune response, participating not only in the early parasite control but also in the pathophysiology of this disease [7–9]. In the chronic phase, two types of parasite-specific antibodies with different functional activities, lytic antibodies (LA) and conventional serology antibodies (CSA) have been described [7,10,11]. LA recognize proteins exposed in the surface membrane of *T. cruzi* infective forms and prompt lysis by antibody-dependent cell cytotoxicity or/and complement-mediated lysis [12–14]. These antibodies are associated with resistance in active ongoing infection but being mainly detected in asymptomatic patients, their presence is further linked to a possible protective response during the chronic phase [12,13,15]. On the other hand, CSA are not associated with parasite resistance, but are useful tools for the serological diagnosis of Chagas disease [11,16]. In addition, infection with *T. cruzi* can lead to the development of host's protein-specific antibodies through different mechanisms like polyclonal B cell activation, organ-specific damage and molecular mimicry [5,9,17–21]. Among the latter, some examples of antibodies to parasite/host proteins are those raised against cruzipain/myosin, cruzipain/cardiac receptors, B13/myosin, Shed Acute Phase Antigen (SAPA) and TENU2845/Cha antigen, calreticulin/calreticulin, skeletal muscle calcium dependent (SRA)/SRA [17,18,22]. It is important to highlight that some of these cross-reactive antibodies might be in part responsible for the pathogenic events underlying this disorder [17,23,24]. In this line of evidence, our group and others demonstrated that patients with chronic Chagas Heart Disease (cChHD) develop antibodies with functional effects on cardiac receptors [25,26]. These mainly recognize the C-terminal end of the *T. cruzi* ribosomal P2β protein (peptide R13, EEEDDDMGFGLFD), which shares similarity to an acidic motif (i.e. sequence AESDE) located on the second extracellular loop of the β1-adrenergic receptor [26,27]. Interestingly, the long-lasting stimulatory activity of anti-P2β antibodies prompt apoptosis in the murine cardiac cell line HL-1 by non-canonical receptor signaling pathways (unpublished results) [28]. Furthermore, cChHD patients with diminished cardiac vagal function and/or colonic denervation syndrome display a high level of antibodies against M2 muscarinic receptors [29,30].

To extend the molecular features of the host humoral immune response against the parasite in a pathological scenario, we previously analysed the repertoire of 125 variable heavy chain (VH) genes from plasma cells isolated from the heart tissue of three subjects with cChHD and from a Fab combinatorial library derived from bone marrow B cells of other cardiac patients [31]. Both, VH genes amplified from cardiac tissue, as well as those from anti-*T. cruzi* Fab library presented a high degree of somatic mutations, suggesting indirect and direct evidence of a parasite antigen driven selection process. Following the same line of investigation, we have constructed single-chain variable fragment (scFv) antibody phage display libraries derived from B-cell mRNA of cChHD patients. Screening the libraries against whole *T. cruzi* lysate allowed us to isolate scFv antibodies with different parasite protein specificity. In the present study, we report the isolation, expression and characterization of one scFv antibody, named A2R1 that recognizes *T. cruzi*'s tubulin and cross-reacts very specifically with a human tubulin isoform occurring in nervous system. Our results disclose a new tissue-specific molecular target of autoreactive antibodies that may be linked to the pathophysiology of Chagas disease.

2. Methods

2.1. Ethics statement

The research protocols were approved by the Medical Ethics Committees of the Hospital General de Agudos Dr. Juan A. Fernández and Hospital General de Agudos José María Ramos Mejía, Buenos Aires, Argentina. All enrolled patients gave written informed consent, according to the Hospital's Ethics Committee guidelines, before sample collection and after the nature of the study was explained.

All animal experiments were carried out in accordance with the Guide of Care and Use of Laboratory Animals, 8th Edition (2011), and the protocols used were approved by Animal Care Committee of the Instituto de Medicina Experimental (IBYME-CONICET).

2.2. Study population

Bone marrow of two subjects (donor #1 and 2) and peripheral blood mononuclear cells of nine subjects (donor #3 to #11) with cChHD were used for the construction of the scFv libraries. Included individuals had a minimum of two positive serological tests for *T. cruzi* infection in compliance with domestic and international criteria [1] and endured cardiac alterations, ascertained after clinical and cardiological examination [31,32].

2.3. Parasites and lysates

Epimastigotes of *T. cruzi* G (DTU Tc I), Y (DTU Tc II), CL Brener (DTU Tc VI) strains [33], *C. fasciculata* and *B. culicis* were grown in liver infusion tryptose (LIT) medium supplemented with 10% fetal bovine serum (FBS, Natocor) at 28 °C. Infective *T. cruzi* metacyclic trypomastigotes obtained from epimastigote cultures were grown and purified by passage through DEAE-cellulose column, as described [34]. *T. cruzi* amastigote and trypomastigote forms were obtained from the culture media of infected HeLa cells (CVCL_0058). The procyclic form of *T. brucei* strain 29–13 [35] was grown in SDM-79 medium (Sigma-Aldrich) supplemented with 10% FBS, 7.5 mg/ml hemin, 100 U/ml penicillin and 100 μg/ml streptomycin at 28 °C. To prepare cell extracts, parasites were lysed in 50 mM Tris–HCl pH 7.5, 250 mM sucrose, 5 mM KCl, 1 mM PMSF, 2 μg/ml leupeptin, 1 mM

benzoamide, 25 U/ml trasylol, protease inhibitor cocktail (Roche). After three rounds of freeze-thawing (liquid nitrogen), protein lysate concentration was determined using the Bradford Protein Assay (Bio-Rad). Lysate from L. *brasiliensis* promastigote was a gift from Dr. E. Bontempi (Instituto Nacional de Parasitología "Dr. Mario Fatala Chaben", Buenos Aires, Argentina).

2.4. Mouse and rat tissue lysates

Organs from 8-week-old C57BL/6 mice and Wistar rats were pulverized in liquid nitrogen and minced in lysis buffer containing 50 mM Tris−HCl pH 7.5, 50 mM NaCl, 1 mM EDTA, 1 mM phenylmethylsulfonylfluoride, 1 mM benzamide, 1% (v/v) Triton X-100, 10% (v/v) glycerol and protease inhibitor cocktail. After centrifugation at 16,000 x *g* for 10 min, protein suspensions were aliquoted, and stored at −80 °C. Lysis buffer for liver and muscle tissues contained 250 mM sucrose and 10 mM EDTA. Protein concentrations were measured with the Bradford Protein Assay.

2.5. T. cruzi *flagellar protein preparation*

T. cruzi epimastigote lysates were spun at 1500 x *g* for 10 min and the pellet extracted once more was then resuspended in high-salt buffer (100 mM Tricine pH 8.5, 1 M NaCl, 1% Nonidet P-40, protease inhibitor cocktail) for 10 min on ice following centrifugation at 300 x *g*. Large aggregates and high molecular weight nucleoproteins were removed from the bottom of the tube by careful aspiration with Pasteur pipette and the remaining solution was centrifuged at 12,000 x *g* for 10 min. The flagellar preparation was kept at −80 °C until use.

2.6. Cell culture and lysates

Embryonic mouse hypothalamus cell line N43/5 (CVCL_D452) was cultured in DMEM medium (GIBCO) supplemented with 10% FBS, 100 U/ml penicillin, 100 μg/ml streptomycin and 2 mM L-glutamine in a humidified 37 °C incubator containing 5% CO_2. Cell lysates were prepared as described previously [36].

2.7. Isolation of the human scFv A2R1

The scFv phage library construction and subsequent selection of antibodies were described elsewhere [31,32,37]. Six scFv phage libraries (VH-VLκ or VH-VLλ) of over 1.2×10^8 clones was finally cloned into *pHenIX* vector and used for selection of human scFv antibodies using cell lysates from *T. cruzi* epimastigotes (CL-Brener). The PCR analysis of the selected phage clones demonstrated that one of the positive anti-*T. cruzi* phage-scFv clones harboured a full-length insert and was named A2R1. A2R1 was subcloned into the expression vector *pUC119-VSV-HIS6* [38].

2.8. Recombinant scFv A2R1 expression and periplasmic purification

Escherichia coli HB2151 cells transformed with *pUC119-VSV-HIS6-A2R1* were grown in 2x tryptone/yeast medium (2xTY) supplemented with 2% glucose and 100 μg/ml ampicillin at 37 °C. After induction with isopropyl−β−d−thiogalactopyranoside (IPTG, final concentration 1 mM) in a medium lacking glucose, the scFv A2R1 was purified using Ni^{2+}-NTA affinity columns according to the manufacturer's instruction (QIAGEN). scFv A2R1 concentration was determined spectrophotometrically (ε_{280nm} = 24,535 $M^{-1}cm^{-1}$) whereas its expression and reactivity were assessed by Western-blot.

2.9. Cloning of chimeric A2R1 antibody

The mouse-human chimeric antibody A2R1 (chim mA2R1) was assembled by cloning the scFv A2R1 heavy (VH) and light chain V (VL) region into mouse C gene segments [39]. Briefly, amplified VH and VL regions were obtained by PCR and sub-cloned into a eukaryotic expression vector containing mouse genomic IgG1 heavy and kappa light chain constant regions and regulatory elements of the immunoglobulin locus. The chimeric expression constructs were transfected into HEK293 cells by electroporation. Secreted chimeric A2R1 full-length antibody was purified from the cell culture supernatants by Protein A chromatography (MabSelect SuRe™, GE Healthcare). The reactivity of chim mA2R1 against *T. cruzi* lysate was tested by Western-blot (Supplementary Fig. 1).

2.10. Expression of recombinant T. cruzi *tubulin*

T. cruzi α-tubulin (TcATUB) was expressed fused to GST (TcATUB-GST) in *E. coli* BL21 cells harbouring the *pGEX-4T-2-alphaTub* vector (generously provided by Dr. S. Schenkman, Universidade Federal de São Paulo, Brazil). After IPTG induction, total protein extracts were prepared, harvesting 1×10^9 cells by centrifugation at 3000 x *g* and disrupted with the addition of 5x SDS-PAGE loading buffer.

TcATUB was expressed in the supernatant of L. *tarentolae* promastigotes using the LEXSY System (Jena Bioscience). The coding sequence for TcATUB was cloned into the expression vector *pLEXSY-hyg2* fused in-frame with a signal peptide for its secretion into the culture medium [40]. Parasite transfection and culture selection were as previously described [41]. Briefly, 1×10^8 L. *tarentolae* cells was electroporated with 30 μg of linear *pLEXSY-hyg2-TcATUB* vector. After culture selection growing parasites in the presence of 100 μg/ml hygromycin B (InvivoGen), supernatant containing the secreted TcATUB was separated from cells by centrifugation at 1500 x *g* for 15 min. Supernatants from recombinant and wild type L. *tarentolae* cultures were fractionated in 200 μl aliquots, mixed with 20 μl 5x SDS-PAGE loading buffer and stored at −20 °C.

2.11. Enzyme-linked immunosorbent assay (ELISA)

ELISA was performed as previously described.[42]. Briefly, either 5 μg/ml BSA or 20 μg/ml of protein lysate from parasite or mouse/rat tissue were coated ON at 4 °C in 0.05 M carbonate buffer (pH 9.6) in 96-well plates (NUNC MaxiSorb). scFv A2R1 (25 μg/ml) was incubated for 2 h at 37 °C and was detected by incubation for 1 h at 37 °C with mouse anti-VSV antibody (1:5000, clone P5D4, Sigma-Aldrich) followed by 1 h at 37 °C with anti-mouse IgG1-HRP (1:3000, Sigma-Aldrich). All antibodies were diluted in 1% (w/v) skimmed milk in PBS containing 0.1% Tween-20 (PBST). In the competition experiment, plates coated with 5 μg/well parasite lysate were incubated with scFv A2R1 (0.02 μg/ml) and 25 μl of *T. cruzi* lysate or mouse/rat whole tissue lysate ranging from 1.25 to 20 μg/ml in 1.5% (w/v) BSA in PBST. Bound scFv was detected by mouse anti-VSV antibody and anti-mouse IgG1-HRP as described above. The reaction was revealed with 3,3′,5,5′-tetramethylbenzidina (TMB, Sigma-Aldrich) or o-Phenylenediamine (OPD, Sigma-Aldrich) and optical density was measured at 450 or 492 nm, respectively using a VERSAmax® ELISA plate reader (Molecular Devices Corportation).

2.12. Western-blot

Proteins were separated on 10−12% SDS-polyacrylamide gels and transferred to nitrocellulose sheets. Membranes were blocked with 3% (w/v) skimmed milk in TBST and then incubated with patient sera (1:5000), scFv A2R1 (25 μg/ml) mixed with mouse anti-VSV (1:5000), rat anti-tyrosinated α-tubulin (1:1000, YL 1/2, Pierce Antibodies), mouse anti- acetylated α-tubulin (1:2000, clone 6−11B-1, Sigma Aldrich), mouse anti-β tubulin (1:1000, CA N3557, Amersham) antibodies or chim mA2R1 (1 μg/ml) for 2 h at RT in 2% (w/v) skimmed milk in TBST (M-TBST). After washing with TBST, membranes were incubated with mouse anti-human IgG1-HRP, rabbit

anti-mouse IgG1-HRP or goat anti-rat IgG-HRP (all diluted 1:3000, Sigma-Aldrich) for 1 h at RT in 2% M-TBST. Immunoreactive bands were visualized by chemiluminescence detection (SupersignalTM West Pico, Pierce) or by colorimetric reaction with TMB.

2.13. Immunoprecipitation and nanolc mass spectrometry

Immunoprecipitations (IPs) were performed on *T. cruzi* epimastigote (CL-Brener) lysates, using chim mA2R1 covalently coupled to NHS-Activated Magnetic Beads (Thermo Pierce Scientific). Briefly, 300 μl of magnetic beads were washed according to the manufacturer's instructions and coupled to 300 μg of chim mA2R1 under rotation for 16 h at 4 °C. After washing twice with 0.1 M glycine pH 2.0 and ultrapure water, reaction was stopped by incubation with 3 M ethanolamine pH 9.0 for 2 h at RT. A total of 50 μl of chim mA2R1 coupled-beads were incubated with 1 mg total protein of *T. cruzi* lysate diluted in PBS for 6 h at 4 °C under rotation. Bound proteins were eluted with glycine pH 2.0 and immediately neutralized with 1 M Tris−HCl pH 9.0. The same procedure was carried out using magnetic beads without chim mA2R1 as negative control. Eluted fractions were resuspended in 10x sample buffer (0.25 M Tris, pH 6.8, 8% SDS, 35% glycerol and 0.2% bromophenol blue), subjected to SDS-PAGE and stained with colloidal Coomassie Blue G-250 (Sigma-Aldrich). The stained protein bands were excised, in-gel digested with trypsin as described elsewhere [43] and subjected to nano-flow reversed-phase LC-MS/MS analysis at the Radboud Proteomics centre, Nijmegen, The Netherlands. MS/MS spectra were converted into mgf files (MSConvert, ProteoWizard, version 3.0.06245) and then analysed using Mascot search engine (http://www.matrixscience.com). Extracted peptides were aligned to the "trypanosomatids" entries in the Uniprot [44] and TriTrypDB databases [45].

Carbamidomethylation of cysteine was specified as fixed modification and oxidation of methionine as variable modification.

2.14. Two-dimensional electrophoresis and mass spectrometry analysis

Two-dimensional (2D) electrophoresis was performed as described by Görg et al [46]. A total of 120 μg of desalted flagellar proteins solubilized in 8 M urea containing 2% (v/v) CHAPS and 20 mM DTT was loaded onto an immobilized pH gradient IPG gel strip 3−11 NL (Immobiline Dry strip, GE HealthCare) and isoelectrofocused subsequently at 500 V for 30 min, 1000 V for 1 h, 2000 V for 1 h, and 5000 V for 7 h. The strips were incubated in equilibration buffer (75 mM Tris−HCl pH 6.8, 6 M urea, 30% (v/v) glycerol, 2% (w/v) SDS, 0.01% (w/v) bromophenol blue) containing 10 mg/ml DTT for 15 min and then in equilibration buffer containing 2.5 mg/ml iodoacetamide for 15 min. Equilibrated strips were placed on 12% polyacrylamide gels, sealed with 0.5% agarose solution, and proteins separated at 4 °C using a Bio-Rad electrophoresis unit. Gels were either blotted onto nitrocellulose membranes for immunoblot analysis as indicated above or stained with colloidal Coomassie Blue G-250. Individual spots were excised from the gel and submitted to the Centro de Estudios Químicos y Biológicos, Universidad de Buenos Aires, Buenos Aires, Argentina for protein identification by MALDI-TOF mass spectrometry. MS/MS spectra were analysed as described previously.

2.15. Immunofluorescence analysis

Washes and compound dilutions were performed in PBS, otherwise indicated.

In parasites: Cells were washed twice, seeded onto poly-lysine coated coverslips for 30 min and fixed with 3.8% (w/v) paraformaldehyde (PFA) for 20 min and permeabilized with 0.1% (v/v) Triton X-100 for 10 min. Coverslips were blocked with 1% (w/v) BSA (blocking solution) for 10 min and then incubated for 1 h with scFv A2R1 (40 μg/ml) mixed with mouse anti-VSV (1:5000) or rabbit anti-His (1:3000, GeneTex), rat anti-α-tubulin tyrosinated (1:1000) or mouse anti-β tubulin (1:1000) antibodies. After thorough washes, coverslips were incubated for 45 min with Alexa488- or Cy3-conjugated goat anti-mouse antibodies (Invitrogen, Thermo-Fisher), Alexa488-conjugated goat anti-rabbit (Invitrogen, Thermo-Fisher) or Cy3-conjugated goat anti-rat antibodies (Jackson Immunoresearch), all diluted 1:1000. Primary and secondary antibodies were used diluted in blocking solution. When appropriate, parasite nucleic acids were stained with 4′,6-diamidino-2-phenylindole (DAPI, 300 ng/ml) for 1 h. The coverslips were thoroughly washed before mounting with DABCO (Sigma-Aldrich) and images were acquired on a Nikon E600 fluorescence microscope coupled to a DXM 1200F digital camera using ACT-1 software or a Nikon C1 Confocal Microscope using the EZ-C1 2.20 software. For cytoskeleton extraction, a fresh culture of parasites was prepared using modified protocol described by Bonhivers et al [47]. Briefly, parasites were washed, then spread on poly-lysine coated coverslips and permeabilized for 5 min with 1% (v/v) NP40 in PIPES buffer (100 mM PIPES pH 6.9, 2 mM EGTA, 1 mM $MgCl_2$). After two washes with PIPES buffer and PBS, preparations were fixed with 4% (w/v) PFA followed by a cold methanol treatment (−20 °C) for 5 min and processed as previously described.

In mammalian cells: N43/5 cells were grown directly on poly-lysine coated glass coverslips and fixed with 3.8% (w/v) PFA for 15 min at 4 °C once they reached a confluence of 70%. Fixed cells were then quenched by washing with 0.02 M glycine for 5 min, followed by permeabilization with 0.1% (v/v) Triton X-100 for 10 min and a subsequent blocking step with 1% (w/v) BSA. Coverslips were incubated with scFv A2R1 mixed with rabbit anti-His-and mouse anti-β tubulin and then with Alexa488-conjugated goat anti-rabbit and Alexa546-conjugated goat anti-mouse (1:1000, Invitrogen, Thermo-Fisher) as primary and secondary antibodies, respectively. Incubation times and dilutions, as well as coverslips mounting were performed as described above for parasites.

In HELA cells infected with T. cruzi: Purified metacyclic trypomastigotes of CL Brener strain were seeded onto each well of 24-well plates containing 13-mm diameter round glass coverslips coated with HeLa cells at a multiplicity of infection of 10:1 (parasite:cells). After 144 h incubation with parasites, the coverslips were fixed with acetone at −20 °C for 15 min, washed and incubated with scFv A2R1 mixed with mouse anti-VSV antibody and Alexa488-conjugated goat anti-mouse as primary and secondary antibodies. Palloidin-rhodamine was used to stain F-actin (Thermo-Fisher). Incubation times and dilutions, as well as DNA staining and coverslips mounting were performed as described above for parasites.

2.16. Cytometry

N43/5 cells were fixed in 2% (w/v) PFA for 15 min at RT and permeabilized in 0.1% (v/v) Triton X-100, 1.5% (w/v) BSA in PBS. After 30 min at RT, cells were incubated sequentially with scFv A2R1 (200 μg/ml diluted in PGN) mixed with mouse anti-VSV (1:5000) and Alexa488-conjugated goat anti-mouse (1:1000) antibodies for 1 h at 4 °C in 1% (w/v) BSA in PBS. Samples were acquired on a FACScan flow cytometer (Becton Dickinson) and data analysis was performed with FlowJo software (TreeStar Inc.).

2.17. Immunohistochemical analysis

Five-μm thick sections of paraffin-embedded tissues from patients with refractory epilepsy or without any apparent pathology were mounted on coated immunoslides (SupaFrost, Thermo Scientific) and dewaxed in xylene, rehydrated in graded ethanol series and treated for 30 min with 3% (v/v) H_2O_2 in 70% (v/v) ethanol to quench endogenous peroxidase activity. After three washes with dH_2O, sections underwent heat antigen retrieval by incubation with 10 mM

citrate buffer pH 6.0 for 50 min at 80 °C. Sections were subsequently blocked with 2.5% (w/v) BSA in PBS for 30 min, and incubated with scFv A2R1 (50 μg/ml) mixed with mouse anti-VSV antibody (1:1000) or sera from donors (1:500) in PBS ON at 4 °C. After washing with PBS, biotinylated goat-anti mouse (1:400, BA-9200, Vector Laboratories) or goat-anti human (1:1000, Sigma-Aldrich) antibodies were incubated for 1 h in the presence of HRP-conjugated Streptavidin (ABC Kit Vectastin, Vector Laboratories) and then washed with PBS. Tissue slides were developed using 3,3′-Diaminobenzidine (DAB, Dako Cytomation, Glostrup) as substrate, washed with dH_2O, counterstained with haematoxylin (Alwik), rinsed with tap water, rehydrated in graded series of ethanol and xylene and covered with permanent mounting medium (Eukitt, Merck). Negative controls were performed by substituting the primary antibody with a control scFv or incubating only with the anti-VSV antibody or with healthy−donor sera. Mouse skin tissues were obtained from Swiss mice infected with *T. cruzi* (strain Tulahuen, DTU-Tc VI) kindly provided by Dr. R. Laguens from Department of Pathology, Hospital Universitario Fundación Favaloro, Buenos Aires, Argentina and slides were processed as described.

2.18. VH and VL sequence analysis

Nucleic acid sequencing was conducted at Centro de Genómica Aplicada (Universidad de Buenos Aires, Argentina). Variable region sequences of H and L chains were analysed with the International Im-MunoGeneTics (IMGT)/V-QUEST alignment tool at IMGT database. Mutations were identified by comparing each sequence with the germline sequence and were defined based on amino acid changes in the VH or VL segment. Replacement (R) mutations were determined in framework regions (FRs) and complementary determining regions (CDRs).

2.19. Comparative analysis of tubulin sequences

Amino acid sequences from *Homo sapiens*, *Rattus norvegicus* and *Mus musculus* tubulins were downloaded from UniProt [44]. Sequences from trypanosomatids were obtained from TriTrypDB [45] by downloading the result of intersecting three filters: one to filter the organisms of interest (*T. cruzi, T. brucei, Leishmania spp*. and *C. fasciculata*), one for the term "tubulin" and the last one for either the term "alpha" or "beta". Afterwards, sequences were cleaned by using a custom python script to exclude those sequences that included terms like "pseudogene", "cofactor", "coatomer", "fragment", "unspecified" or "uncharacterized". Finally, sequences with 100% identity were collapsed into single entries. Sequence alignments were generated with Clustal Omega [48] and subsequently hand curated. Identity and similarity percentages were calculated with the tool "Ident and Sim" from the "Sequence Manipulation Suite" using the default parameters [49].

Supplementary Table 1 compiles all the sequences that were used in this study.

2.20. Statistics

Statistical analysis was performed with One-way analysis of variance, followed by a post hoc Tukey test, using GraphPad Prism 5.0 software (San Diego, CA). Data were considered statistically significant at $P < 0.05$. All error bars represent the SD of the mean.

2.21. Role of funding source

This work was supported by grants from Consejo Nacional de Investigaciones Científicas y Técnicas (CONICET; PIP Number 112-2015010-0547 to KAG) and Agencia Nacional de Promoción Científica y Tecnológica, Argentina (ANPCyT; PICT Numbers 2010-2439 and 2014-1026 to KAG and 2016-1028 to MP). The funders had no role in study design, data collection, data analyses, interpretation, or writing of the report.

3. Results

3.1. V-gene sequences and specificity of scFv A2R1

Five scFv phage-display libraries were constructed from B cell cDNA of cChHD subjects by cloning antibody variable domains into the *pHENIX* phagemid vector. After rounds of selection using *T. cruzi* epimastigote lysate as antigens, scFv A2R1 was selected, subcloned into the *pUC119* bacterial expression vector fused with both a His- and a VSV- tag for detection and purification, and transformed in the *E. coli* non-suppressor strain, HB2151. The expected size of the amplified VH and VL (~450 and 350 bp, respectively) as well as the assembled scFv constructs (VH-linker-VL, ~900 bp) was assessed by PCR (Fig. 1a). Western-blot analysis using an anti-VSV antibody revealed a band of ~29 kDa in a sample of recombinant scFv expressed and purified from *E. coli* (Fig. 1b).

Further, we analysed the primary sequence of the antibody based on the IMGT database (Fig. 1c). A comparison with the sequences of germline VH and VL genes showed that the clone A2R1 heavy chain belongs to the VH3−73•01 family, while the light chain belongs to IGLV1−47•01 family-derived germline. The total numbers of replacement mutations (R) of framework and CDRs as well as CDR3 length are summarized in Table 1. The number of different amino acids from germline varied from 17 amino acids in the VH framework (except CDR3) and 16 amino acids in the light chain, suggesting that scFv A2R1 arises from antigen-driven clonal expansion. Interestingly, VH CDR3 contains two cysteine residues which could be part of a loop likely contributing to increase its antigen-binding capacity [50].

In order to test the specificity and reactivity of scFv A2R1, a Western-blot analysis was performed on the different life stages of *T. cruzi*: amastigotes (replicative intracellular form, mammal-stage), trypomastigotes (blood-borne, mammal-stage) and epimastigotes (non-infective, insect-stage) of the CL Brener strain. For all tested parasite's stages, a ~50 kDa band was detected (Fig. 1d), which showed highest and lowest abundance in trypomastigotes and amastigotes, respectively. In addition, the same MW band of ~50−55 kDa was detected in protein lysate from trypomastigotes of Y and G *T. cruzi* strains, and other trypanosomatids like *Trypanosoma brucei, Crithidia fasciculate, Blastocrithidia culicis* and *Leishmania braziliensis* (Supplementary Fig. 2). Of note, the bands with MW <50 kDa likely correspond to partial degradation or changes in post-translational modifications (PTMs) of the ~50 kDa antigen (Fig. 1d and Supplementary Fig. 2).

Moving forward to identify the cellular distribution of the scFv A2R1 antigen, fixed-permeabilized parasites were prepared for immunofluorescence assays. A positive staining was visible along the entire cell body and the flagellum of all parasite forms (Fig. 1e). Consistent with our immunoblotting results, the trypomastigote and epimastigote displayed considerably stronger fluorescence signal intensity than the amastigote. Interestingly, we also noticed that much of the total staining seems to be concentrated in the flagellum and the flagellar pocket when compared to the rest of the parasite body (Fig. 1e).

Overall, our results demonstrated that scFv A2R1 recognizes an intracellular protein highly conserved among strains and developmental stages of *T. cruzi* as well as in other Trypanosomatidae family members.

3.2. Identification of A2R1 antigen

Next, we aimed to identify the protein recognized by scFv A2R1 by using two methodological approaches, immunoprecipitation (IP) and two-dimensional (2D) electrophoresis followed by mass spectrometry analysis.

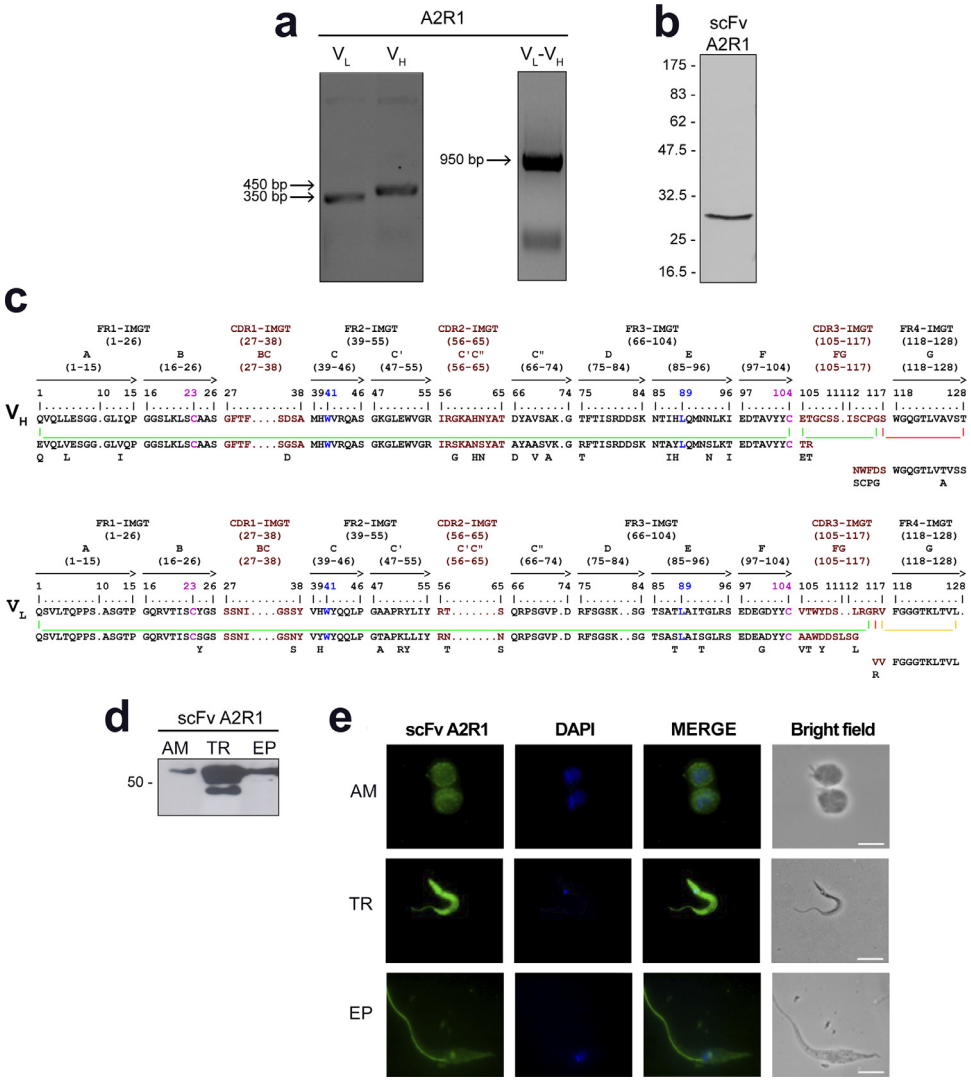

Fig. 1. Features of anti-*T. cruzi* A2R1 antibody isolated from scFv immune phage display libraries constructed from B cells of patients with cChHD. (a) Agarose gel electrophoresis (2%) of PCR amplified products of heavy chain (VH) and light chain (VL) genes and A2R1 gene. Fragment sizes are indicated on the left. (b) Western-blot analysis of periplasmic expression of scFv A2R1. Molecular weight markers (in kDa) are shown on the left. (c) Comparison of VH and VL sequences of scFv A2R1 with their respective human germline sequences according IMGT. FWR: framework; CDR: complementarity determining region. (d) Western-blot of total lysates from *T. cruzi* and its different stages with scFv A2R1. Total cell lysates (30 μg) of amastigote (AM), trypomastigote (TR) and epimastigote (EP) were loaded in each lane and processed by immunoblotting. Molecular weight markers (in kDa) are shown on the left. (e) Immunofluorescence of different stages of *T. cruzi* incubated with scFv A2R1 (green) and counterstained with DAPI (nucleic acid stain, blue). The third and fourth columns show the merged and bright field images of the parasites, respectively. Scale bar: 0.5 μm.

Since the human scFv A2R1 was selected from a panning against whole detergent soluble epimastigote lysate, proteins from this cell extract were subjected to IP using a chimeric A2R1 antibody containing murine IgG1,k constant domains and the human scFv A2R1 variable domains (chim mA2R1). It should be pointed out that the rationale behind undertaking this experimental procedure with a full length antibody instead the single chain fragment was merely based on the performance of the IP assay. Among the numerous proteins pulled down with chim mA2R1 (Fig. 2a), a major band of the expected MW (50–55 KDa) was observed in the antibody-containing sample and was absent in the negative control. The identity of this band was assessed using peptide mass fingerprinting (LC-MS/MS), which yielded a total of 19 and 20 peptides corresponding to *T. cruzi* α- and β-tubulin, covering from 44% to 59%, respectively of the hit sequence (Table 2).

Consistent with our finding, we decided to confirm protein identity by carrying out the 2D electrophoresis using a tubulin enriched fraction from *T. cruzi* epimastigotes. Therefore, parasite flagellar preparation which includes the structural axoneme (9 + 2), the associated PFR and the basal body was separated by 2-DE gels using pH 3–10 immobilized pH gradient strips and analysed by colloidal Coomassie Blue G-250 staining and immunoblotting with scFv A2R1 (Fig. 2b). The identity of the selected spots was determined by MALDI-TOF/MS. A 45–65 kDa cluster on the acidic region was divided into 3 spots, each of which was identified as β-tubulin, suggesting the presence of different protein isoforms (Fig. 2b and Table 3).

To test whether scFv A2R1 specifically binds to parasite tubulin, recombinant *T. cruzi* α-tubulin (TcATUB) was expressed in *E. coli*

Table 1
VH and VL gene sequences of scFv A2R1.

V germline Family/ locus	CDR3 sequence	CDR3 length	Number of somatic mutations (aa)
HV3–73•01	ETGCSSISCPGS	12	17
LV1–47•01	VTWYDSLRGRV	11	16

aa= number of amino acid in VH/VL genes compared to germline genes (VL including CDR3; VH excluding CDR3).

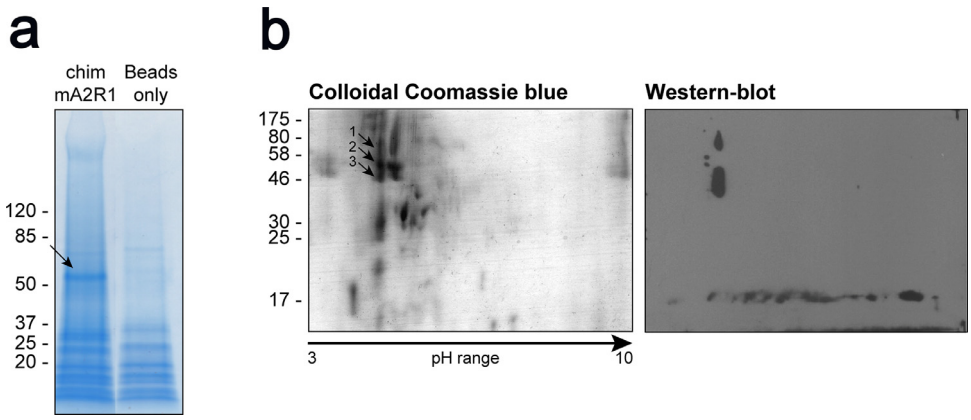

Fig. 2. Identification of A2R1's target antigen. (a) Parasite lysate was immunoprecipitated with chim mA2R1 covalently coupled to NHS-Activated magnetic beads or beads only (negative control). Bound proteins were eluted and subjected to SDS-PAGE (12%), followed by protein staining using colloidal Coomassie Blue G-250. The arrow indicates the band excised and subjected to LC–MS/MS analysis. (b) The 2-D gel of *T. cruzi* flagellar proteins was stained with colloidal Coomassie Blue G-250 (left panel) or transferred to nitrocellulose and revealed with scFv A2R1 (right panel). The arrows denote the spots analysed by MALDI-TOF. Molecular weight markers (in kDa) are indicated on the left.

Table 2
Identification of A2R1 binding protein by immunoprecipitation and mass spectrometry.

Accession number	Protein Description	*In silico* MW (in Da)	Best Mascot Identity score	Sequence coverage (%)
Q27352	Tubulin alpha chain	49,728	26.7	58.1
P08562	Tubulin beta chain	49,573	34.4	44.3
Q7Z1V1	Sterol 14-alpha demethylase	54,683	35.6	19.1
Q4E657	ATP-dependent 6-phosphofructokinase	53,566	28.8	18.1
Q4E162	Probable eukaryotic initiation factor 4A	45,504	35.1	15.1
P33447	Tyrosine aminotransferase	46,167	35.0	7.2
P31072	6-phosphogluconate dehydrogenase	52,155	32.9	4.8

The band corresponding to a MW ~ 50 KDa was cut from the gel shown in Fig. 4A and subjected to LC-MS/MS analysis. Protein identification was achieved through Uniprot and TriTrypDB databases. [45] All theoretical molecular weight (MW) values were calculated using the ExPASy Compute MW/pI tool online. Only proteins belonging to *T. cruzi* and MW between 45,500 and 55,000 are listed.

Table 3
Identification of A2R1 binding protein by 2D electrophoresis and mass spectrometry.

Spot number	Accession number	Protein description	Best Mascot Identity Score	Sequence Coverage (%)	*In silico* data MW (in Da)	Pi
1	P08562	β-tubulin	165	50	49,572	4.69
2	AAL75956	β-tubulin	150	51	49,700	4.74
3	AAL75956	β-tubulin	139	40	49,700	4.74

Spots were excised from the 2-D gel shown in Fig. 4B and analysed by MALDI-TOF mass spectrometry. Protein identification was achieved through Uniprot and TriTrypDB databases. [41,42] All theoretical molecular weight (MW) and isoelectric point (pI) values were calculated using the ExPASy Compute MW/pI tool online.

(Eca) and assayed by Western-blot. Strikingly, scFv A2R1 was unable to recognize the 79 kDa protein band corresponding to the fusion protein TcATUB-GST (Fig. 3a). Thus, we hypothesized that the target epitope would require post-translational modifications (PTMs) carried out by the eukaryotic parasite but not by bacteria [51,52]. To confirm our hypothesis, recombinant TcATUB was produced in the kinetoplastid *Leishmania tarentolae*. In order to avoid cross-reactivity with the endogenous tubulin, TcATUB was expressed in the supernatant of L. *tarentaole* cultures by cloning its sequence fused to a secretory signal. scFv A2R1 detected a major protein band of ~50 kDa in parasite supernatants expressing the secreted TcATUB (LtA) (Fig. 3A). This strong 50 kDa signal was absent in samples from wild type L. *tarentolae* supernatants (LtW). Instead, a fainter protein band of a slightly lower apparent MW was detected in both recombinant and wild type parasite supernatants, which may be due to cross-reactivity of scFv A2R1 with small traces of endogenous L. *tarentolae* tubulin, coming from cell debris not removed by centrifugation. A commercial anti-α-tubulin antibody also recognized a single 50 kDa protein band in supernatants from L. *tarentolae* expressing the secreted TcATUB (Fig. 3b). This antibody also detected a 50 and a 79 kDa protein bands in cell extracts from *T. cruzi* or *E. coli* expressing recombinant TcATUB-GST, respectively. Notably, an antibody directed against acetylated α-tubulin behaved as scFv A2R1, being able to recognize only the antigen produced by a eukaryotic expression system (Fig. 3c). Overall, our results clearly demonstrate that the target antigen of scFv A2R1 is tubulin and that its epitope is likely enriched in N-acetylated residues.

Finally, because the B cell libraries were pooled before selection it was not possible to closely determine whether scFv A2R1 was rescued from B cells of single or different donors. To address this issue, we analysed sera reactivity against TcATUB produced in L. *tarentolae* by Western-blot. Tested at identical dilutions, the serum from donor #2 showed a stronger reactivity than the serum from patient #1 (Fig. 3d), while no signal was detected for the sera from donor #3 to #11 (Supplementary Fig. 3). Given that one of the drawbacks of phage display is that the heavy- and light-chain pairing may not always resemble the natural repertoire of immunoglobulin [53], our results not only suggest that donor #2 could be the main source of this scFv,

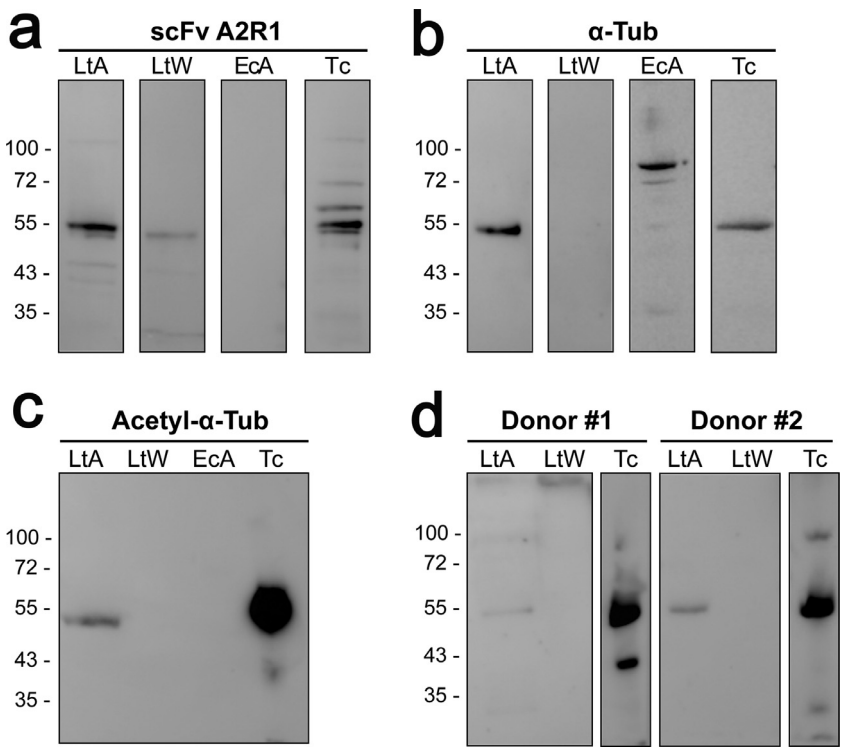

Fig. 3. Reactivity of scFv A2R1 against tubulin expressed in L. *tarentolae*. Western-blot of samples corresponding to the supernatant of L. *tarentolae* expressing TcATUB (LtA; 20 μl), supernatant of wild type L. *tarentolae* (LtW; 20 μl) and total extracts from *T. cruzi* (Tc; 3.5 μg) or *E. coli* expressing TcATUB-GST (EcA; 2 μg). The nitrocellulose membranes were incubated with scFv A2R1 (a), anti-α tubulin (α-Tub) (b), anti-acetylated α-tubulin (Acetyl-α-Tub) antibodies (c) or sera from donor #1 and #2 (d). Molecular weight markers (in kDa) are indicated on the left.

but most importantly demonstrate the existence of anti-tubulin antibodies in the sera of infected patients.

3.3. *Colocalization of scFv A2R1 with commercial anti-tubulin antibodies in* T. cruzi

In order to test that scFv A2R1 and the commercial anti-α and β-tubulin recognize the same subcellular structure/molecular target, we carried out co-localization assays using confocal microscopy. First, we confirmed by Western blot that the commercial antibodies detect a protein band with MW similar to that recognized by scFv A2R1 in *T. cruzi* extracts (Fig. 4a, right panel). Next, immunofluorescence assays showed that scFv A2R1 in permeabilized *T. cruzi* epimastigotes co-localized with the signal of anti-tubulin antibodies, all of which labelled the flagellum and the sub-pellicular microtubules throughout the cell body (Fig. 4a). To study the flagellum structure, the parasites were treated with detergent to remove the cell membrane and soluble proteins, followed by depolymerization of the subpellicular array, leaving the flagellum cytoskeleton intact. Fig. 4b shows that the basal body which is firmly attached to the mitochondrial DNA (kinetoplast) and the flagellum, in its whole length, were recognized by scFv A2R1 and anti-α- and β-tubulin antibodies in samples from epimastigote *T. cruzi* parasites.

3.4. *Recognition of A2R1's target in* T. cruzi*-infected cells*

The capability of scFv A2R1 to recognize parasite tubulin was also evaluated in a more physiological scenario of host-cell infection. Human carcinoma-derived epithelial (HeLa) cells were incubated with the trypomastigote metacyclic forms of CL Brener and after 144 h post-infection were fixed and stained with scFv A2R1. Immunofluorescence images showed that the antibody labelled the intracellular amastigotes on fixed-permeabilized preparations (Fig. 5a). It is worth noting that scFv A2R1 did not react against any structure or cytoplasm of HeLa cells.

Furthermore, immunohistochemistry performed in samples from murine skin chagoma revealed that scFv A2R1 recognized intracellular amastigotes of Tulahuen strain and lacked reactivity towards the mammalian dermal and epidermal cell layers (Fig. 5b).

Collectively, our results clearly show that scFv A2R1 has the ability to tag *T. cruzi* tubulin expressed in different parasite strains and more importantly in the context of *in vitro* and *in vivo* infections.

3.5. *Cross-reactivity of scFv A2R1 with host neuronal protein*

In light of our previous findings but given that tubulin is a highly conserved protein with different isotypes among species [54], we wondered whether scFv A2R1 would recognize any of its mammalian counterpart. For this purpose, we evaluated the reactivity of scFv A2R1 against multiple murine tissue extracts by ELISA and Western-blot. As shown in the upper panel of Fig. 6a (ELISA test), scFv A2R1 displayed a preferential binding to samples from whole rat brain and cerebellum as well as from mouse brain and its different areas, while no significant reaction was observed against any other tissues. Bands of similar MW (~50−55 kDa) to those recognized by scFv A2R1 in *T. cruzi* and other trypanosomatids (Fig. 1d and Supplementary Fig. 2), were detected in whole brain lysates but not in samples from a manifold of rat tissues or parts of murine brain (Fig. 6a, lower panel). The disparity between ELISA and Western-blot assays in A2R1 reactivity could be ascribed to the major features of each assay (i.e. sensitivity), but also to the relative abundance of the neuron-specific tubulin targeted for the antibody in the different organs. Competition ELISA revealed that similar to the inhibition exerted by *T. cruzi* extracts, different concentrations of rat and mouse brain lysate precluded binding of scFv A2R1 to *T. cruzi* protein extract. No competition was achieved with non-brain murine tissue extracts (Fig. 6b).

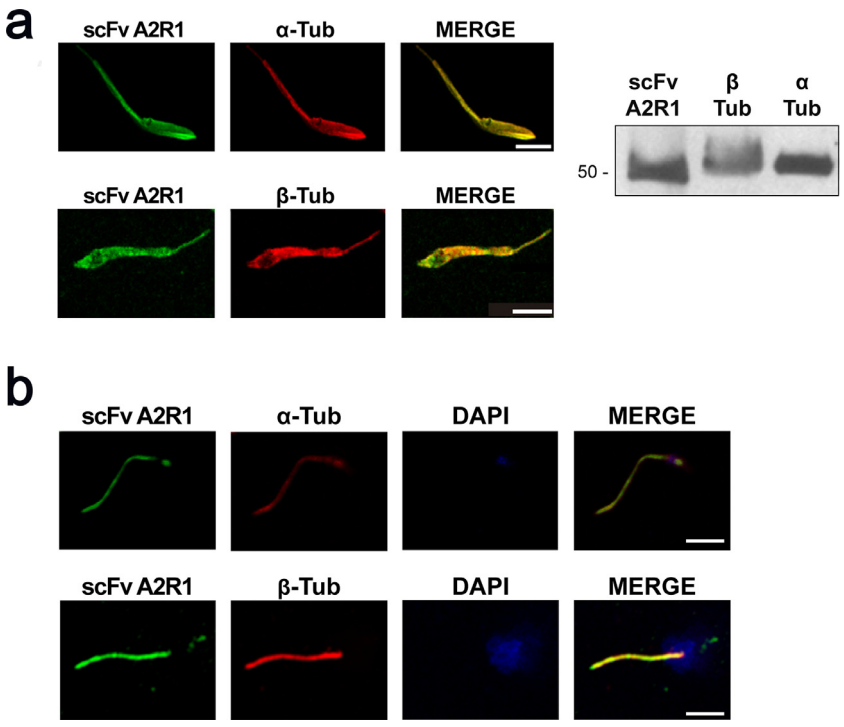

Fig. 4. Co-localization of scFv A2R1 with anti-α/β tubulin antibodies in *T. cruzi*. (a) Confocal microscopy of *T. cruzi* epimastigotes parasites incubated with scFv A2R1 (green, first column) and rat anti-α tyrosinated (α-Tub) or mouse anti-β tubulin (β-Tub) antibodies (red, second column). The third column shows the overlay image. Right panel: Western-blot showing that both commercial antibodies recognize a protein of ~50 kDa presented in parasite lysate (30 μg/lane). (b) Detergent-extracted flagella from *T. cruzi* epimastigotes were co-stained with scFv A2R1 (green, first column), α- or β-tubulin antibodies (red, second column) together with DAPI (blue, third column). The fourth column shows the overlay image. Scale bar: 0.5 μm.

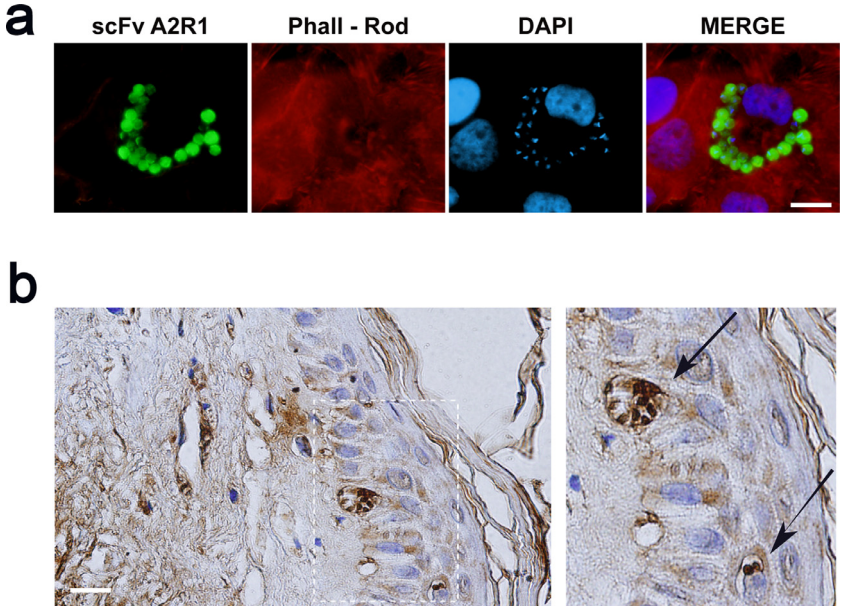

Fig. 5. Reactivity of scFv A2R1 with *T. cruzi* in infected cells. (a) Representative immunofluorescence of HeLa cells infected with *T. cruzi* and incubated with scFv A2R1 (green). DNA and actin filaments staining were performed with DAPI (blue) and phalloidin-rhodamine (red), respectively. Scale bar: 0.5 μm. (b) Immunochemistry assay of mouse skin tissue infected with *T. cruzi* amastigotes (Tulahuen strain). The arrow shows the scFv A2R1 signal. Upon DAB staining, sections were counterstained with haematoxylin. Scale bar: 50 μm.

In line with these results, scFv A2R1 reacted against embryonic hypothalamus murine cells (cell line N43/5) as assessed by immunofluorescence and flow cytometry analysis of fixed-permeabilized samples. Importantly, scFv A2R1 and anti-β tubulin antibody staining showed a near 100% overlap at subcellular level (Fig. 6c). These results suggest that certain antibodies raised in patients during *T. cruzi* infection can recognize a host protein, most likely tubulin, expressed in the brain.

3.6. Ex-vivo *staining of neurons in human brain and gastrointestinal tract samples with scFv A2R1*

The cross-reactivity of scFv A2R1 against proteins expressed in murine brain, encouraged us to evaluate whether this antibody binds to human nervous tissue. Immunohistochemical studies on paraffin-embedded tissue sections of human brain cortex, diencephalon and frontal lobe tissues revealed that scFv A2R1 recognized specifically

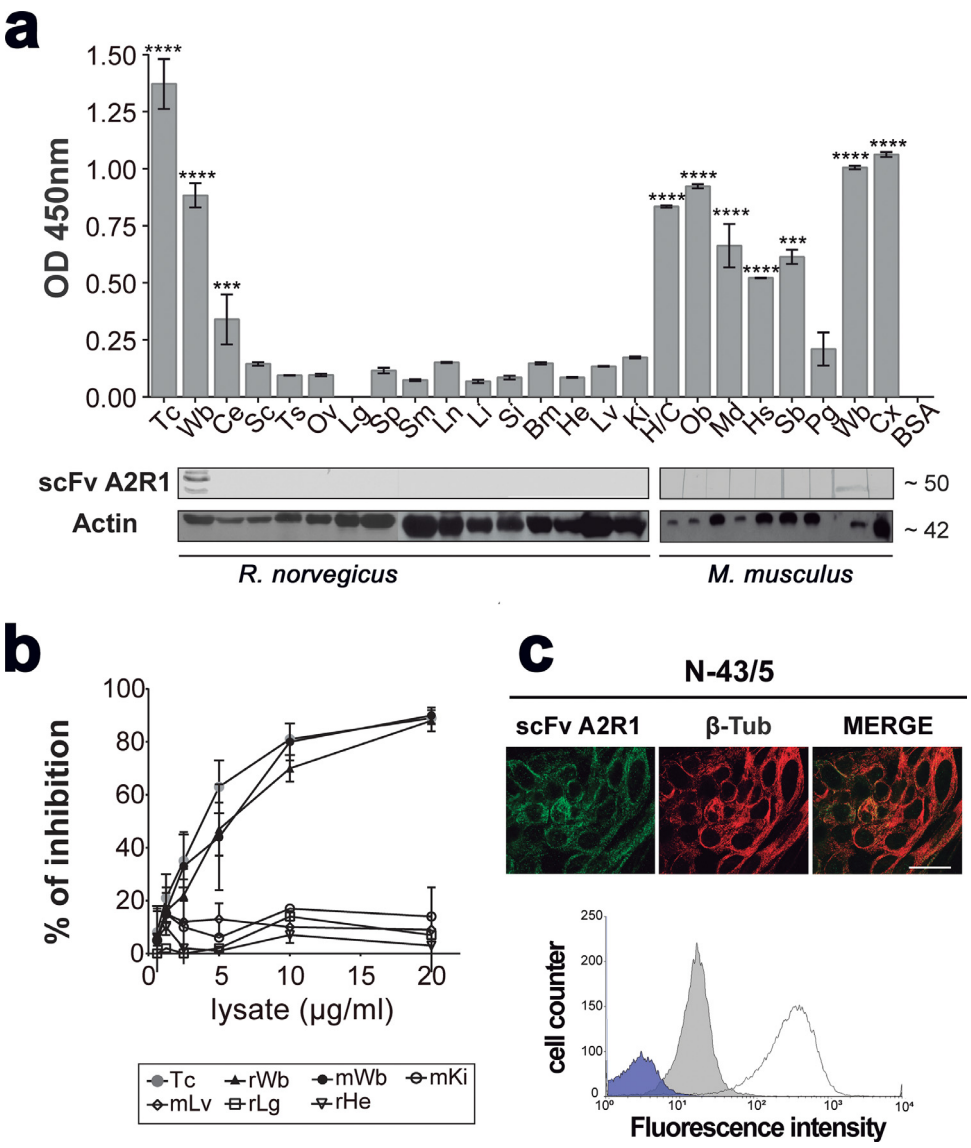

Fig. 6. Reactivity of scFv A2R1 against mammalian tissues. (a) Binding of scFv A2R1 against rat (r) and mouse (m) organ tissue extracts or *T. cruzi* lysate (Tc) evaluated by ELISA (upper panel) and Western-blot (lower panel). The data are expressed as the $OD_{450\ nm}$ (means ± SD; $n = 3$). Differences between means of binding to different lysates vs to BSA were evaluated by one-way ANOVA followed by Tukey's multiple comparison tests. **** $P < 0.0001$; *** $P < 0.001$. For Immunoblotting, 30 μg of protein corresponding to different rat or mouse organ tissue lysate was loaded per lane. The expression of actin was used as a loading control. Molecular weight markers (in kDa) are indicated on the right. Wb: whole brain; Ce: cerebellum; *Sc*: spinal cord; Bm: bone-marrow; Ki: kidney; Sp: spleen; Lv: liver; He: heart; Lg: lung; Li: large intestine; Si: small intestine; Sm: skeletal muscle; Ln; lymph node; Ov: ovary; Ts: testis; H/C: hippocampus/cortex; Cx: cortex; Ob: olfactory bulb; Md: midbrain; Hs: hypothalamus; Sb: striated body; Pg: pituitary gland. (b) Competition ELISA performed with *T. cruzi* proteins coated-plates in the presence of increasing concentrations of mouse (m) and rat (r) organ tissue extracts. Results are expressed as mean percent inhibition values ± SD ($n = 3$). (c) Upper panel: Immunofluorescence of embryonic hypothalamus murine cells (cell line N43/5) using scFv A2R1 (green) and anti-β tubulin antibody (red). Scale bar: 0.5 μm. Lower panel: Representative histograms showing fixed-cells incubated with scFv A2R1 and mouse anti-VSV antibodies (gray line), with anti-VSV antibody only (solid gray) or unstained as negative control (solid blue).

the soma, axon, and dendrite of stellate and large pyramidal neurons (Fig. 7a-d). No positive staining was detected in non-neuronal cells, i.e. astrocytes, oligodendrocytes, and microglia. Since patients with chronic Chagas disease often develop lesions in the sympathetic and parasympathetic peripheral nervous systems, we further investigated the reactivity of scFv A2R1 against different tissues from the gastrointestinal tract, including the esophagus, cecal appendix as well as right and left colon. Immunoreactivity was detected in the neurons arranged in the myenteric (Auerbach's) and the submucosal (Meissner's) plexuses and ganglions (Fig. 7e-h). As seen before, other cellular types, i.e. epithelial cells, immune system cells and connective tissue did not stain with the antibody.

Finally, sera from B cells donors were tested for their immunoreactivity against human brain sections. Consistent with data shown in Fig. 3d, results displayed that only the serum from donor #2 positively stained the diencephalon (Fig. 7i), confirming the existence of this cross-reactive antibody in the serum of this patient. In these experiments, samples of murine chagoma (skin) were used as positive controls while sera from non-infected donors were included as negative controls (Fig. 7j-k, respectively).

Altogether, these data suggest a possible pathogenic role of cross-reacting anti-*T. cruzi* tubulin antibodies in the development of chronic Chagas disease.

3.7. Protein sequence analysis of trypanosomatid and mammalian tubulins

Based on our results pointing out to a neuron specific cross-reaction of A2R1 antibody with tubulins, we compared α- and β-tubulin protein sequences from mammals and parasites, with special

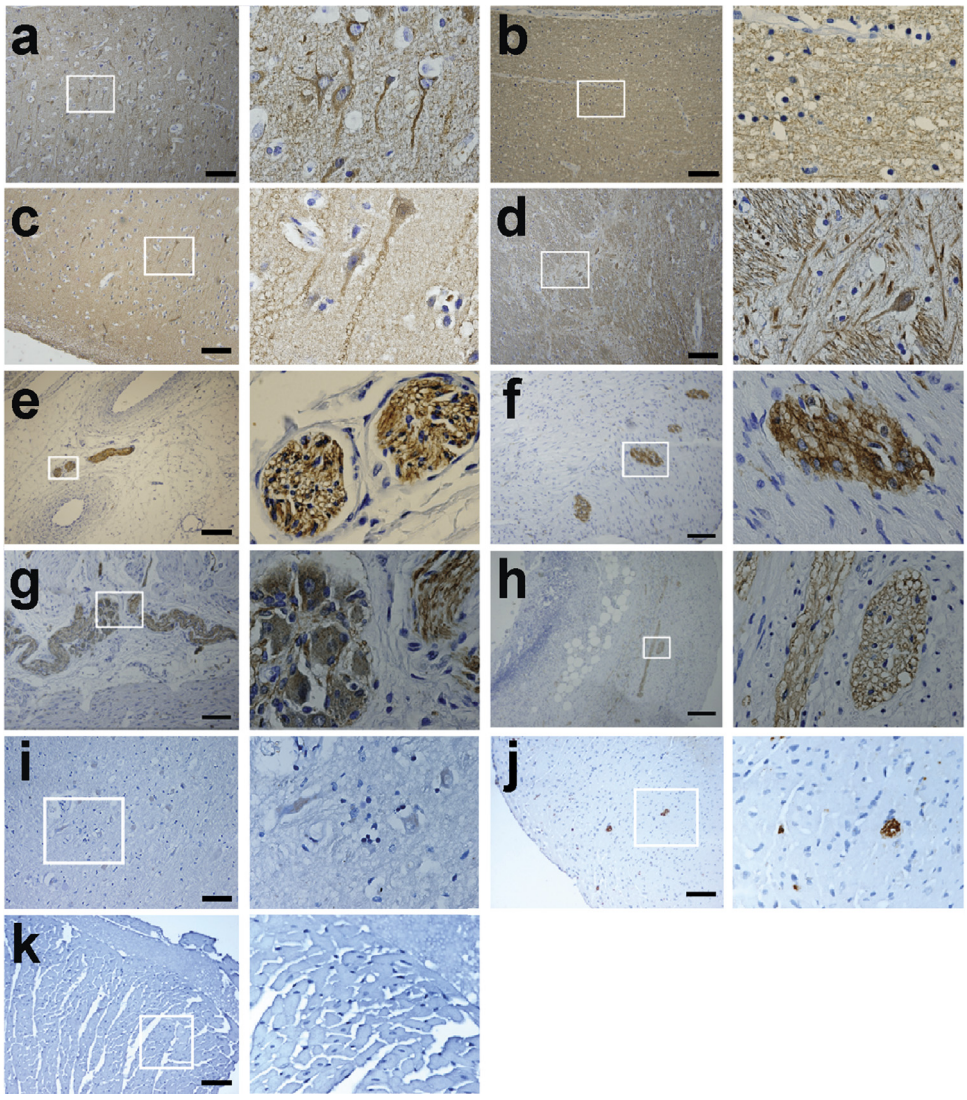

Fig. 7. Immunohistochemical staining of human brain and peripheral nervous system. Representative images of paraffin-embedded sections of tissues from refractory epilepsy patients or healthy individuals challenged with scFv A2R1 and sera from donor patients. After deparaffinization, tissue sections were incubated with scFv A2R1 (a-h; j), serum from donor #2 (i) or from a non-infected donor (k). Tissue coverslips were developed with DAB as a substrate and counterstained with haematoxylin. Scale bars: 100 μm (left column); 200 μm (inset in right column). A: temporal lobe; B: frontal lobe; C: hippocampus; D: diencephalon; E: left colon; F: right colon; G: esophagus; H: cecal appendix; I: olfactory bulb; J: skin of murine chagoma provoked by *T. cruzi* Tulahuen strain (positive control); K: left colon (negative control). No staining pattern was observed with sera from other donors that were included to prepare the scFv libraries.

emphasis on PTM sites. An alignment was built with tubulin sequences from mammals (human, rat and mouse) plus 100 α-tubulin and 83 β-tubulin sequences from the parasites *T. cruzi, T. brucei, C. fasciculata* and *Leishmania spp*. Mammalian α- and β-tubulins have different isotypes that can be mainly distinguished by their C-terminal sequences [52,55,56], while trypanosomatids display a single isotype for α-tubulin and another one for β-tubulin (Fig. 8). The sequence identity between trypanosomatids tubulin is ~95–99% and ~70–85% when compared to the mammalian counterparts (Supplementary Table 2). Furthermore, trypanosomatid α-tubulin possesses the highest identity and similarity with mammalian isotypes 1 and 3 while β-tubulin is similar to the isotypes 2, 4 and 5.

Protein aligned sequences showed that all PTM sites found in the N-terminal and intermediate domains of mammalian tubulin are conserved among the trypanosomatid tubulins (Fig. 8), except for α-tubulin's polyamination site, Glutamine 128, that is also absent in the mammalian isoforms TUBA3C/D/E and TUBA8. Regarding the C-terminal PTMs, the sequences from trypanosomatid tubulins exhibit multiple glutamic acids that can undergo polyglutamylation [52,57]. Interestingly α- and β-tubulins from trypanosomatids present a C-terminal tyrosine, contrary to mammalian tubulins where only α-tubulin's isotypes 1 and 3 harbor this residue at their C-terminal ends (Fig. 8). This might indicate that in trypanosomatids, both α- and β-tubulins can be detyrosinated [52].

Overall, our analyses show high identity and similarity among the sequences of parasites and mammals, and a complete conservation in trypanosomatids of all PTM sites previously reported in mammalian α- and β-tubulins.

4. Discussion

Herein we report for the first time the characterization of a human monoclonal antibody isolated by using the single-chain Fv phage display library technology that specifically recognizes both *T. cruzi* and human tubulins. The scFv libraries were constructed by amplifying the immunoglobulin genes from chronic Chagas disease patients and were panned using a protein lysate of non-infective *T. cruzi* epimastigotes. The isolated antibody, named A2R1, binds to tubulin present in the three life stages of *T. cruzi*, as well as in other members of the *Trypanosomatidae* family such as *T. brucei*, L. *braziliensis, C. fasciculata*

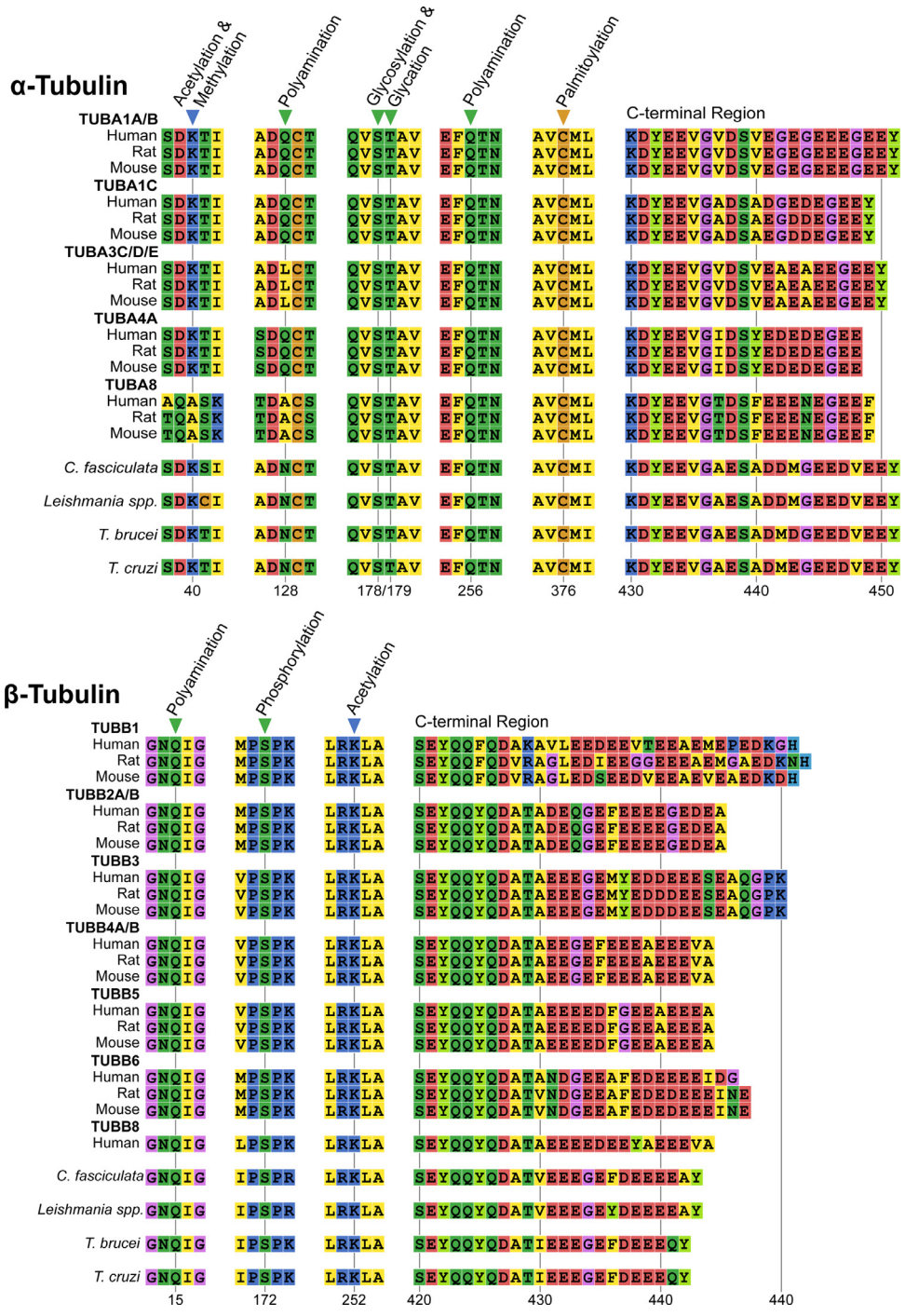

Fig. 8. Multiple sequence analysis of post-translational modification sites and C-terminal regions of tubulin from mammals and trypanosomatids. Sequence alignment corresponding to the PTM sites (+/- 2 amino acids) and C-terminal regions of α- and β-tubulins from mammalian isotype and trypanosomatid chains. Multiple sequences were aligned for the trypanosomatid α- (N = 100) and β- (N = 83) tubulins, but as the featured regions show 100% conservation, only a single sequence is being displayed. The amino acid positions are displayed below the aligned sequences.

and *B. culicis*. Notably, the antibody reveals a significant degree of cross-reactivity with human tubulin expressed in neurons, but not in supporting cells from the peripheral and central nervous system.

Tubulin is a highly conserved globular protein found in solution as heterodimers of two closely related 55-kDa polypeptides, α-tubulin and β-tubulin [58–60]. In mammalians, the tubulin consists of seven α- and eight β-tubulin isotypes which have different functionalities as well as tissue distribution [61]. To date, only one isotype of α- and β-tubulin has been described in trypanosomatids. [52] The tubulins from both organisms differ mostly in the length and primary sequence of the highly negatively charged and disordered C-terminal tail which is exposed at the protein surface. This region undergoes the majority of the PTMs [62–65]. Tubulin polymerization forms the protofilaments that, via a dynamic process, assemble into microtubules, one of the major components of the cytoskeleton with key roles in maintenance of cell shape, motility, trafficking of proteins and organelles as well as in the formation of mitotic spindle during cell division [66]. In trypanosomatids, the microtubules are involved in the morphological changes occurring during the parasite life cycle [67].

Previous studies reported the occurrence of antibodies against tubulin in murine infection models of *T. cruzi* [68–72]. By analysing the antibody repertoire with a semiquantitative immunoblot, Montalvão et al. identified tubulin as the major protein antigen of mice acutely and chronically infected with *T. cruzi* clone Dm28c [72]. Interestingly, monoclonal antibodies obtained from a mouse infected with a clinical isolated *T. cruzi* strain, recognized parasite tubulin and α- but not β-tubulin isolated from chicken brain extracts [68,69]. However, the tissue-specificity of these antibodies was not further studied. On the other hand, antibodies reactive to neurons of the central and peripheral nervous system [73] as well as sciatic nerve homogenate [74] have been found in sera from patients with chronic Chagas disease. Herein, the cross-reactivity of A2R1 with host tubulin expressed in specific structures of the nervous system is demonstrated by the following observations: *i*) A2R1 reacted against brain lysate or its different sections; *ii*) A2R1 signal co-localized with that of anti-tubulin antibodies in a neuroblastoma cell line; *iii*) A2R1 yielded positive immunohistochemical staining of neuronal cells from human brain and different tissues of the gastrointestinal tract and *iv*) A2R1 did not recognize any structure of HeLa cells, skin from murine chagome or immune/supporting cells from neuron tissue. Although polyclonal B lymphocyte activation or hypergammaglobulinemia are two phenomena directly associated with the infection [6,75,76], molecular mimicry is the leading hypothesis for the existence of self-reactivity against tubulin in the context of Chagas disease. Molecular mimicry arises from four well-described types of events, namely a complete identity, homology, shared-epitopes or structural similarities between host's and pathogen's proteins [77]. Our findings clearly are in line with the third type of event since A2R1 recognizes a tubulin epitope modified by one of the PTMs described in trypanosomatids [52]. These data and the fact that some isotypes of mammal's tubulins are neuron specific (TubB3 and TubB4A) [55] raise the question about the structural motif of tubulin that is recognized by the antibody. Our *in silico* analysis of all the human and trypanosomatids α- and β- tubulin protein sequences available in public databases [44,45,78–80] could not provide conclusive information because most residues subject to PTM (i.e. acetylation, detyrosination/tyrosination, polyglutamylation) are conserved among the different species. Of note, tubulin phosphorylation can be ruled out because tubulin dephosphorylation occurs upon adhesion of trypomastigotes to the extracellular matrix [81], and A2R1 did recognize the parasite in the murine chagoma. However, the fact that tubulin acetylation and tyrosination have a main role in the development of neurodegenerative diseases [82,83], tempt us to speculate that the target epitope may contain these PTMs. Currently, we are in the process of challenging our hypothesis by dissecting the molecular specificity of antibody recognition.

Regarding the neurological manifestations in Chagas disease, they are detected in up to 10% of patients in the acute phase, and include meningoencephalitis, headaches, tumor-like form, lethargy and mood changes [84,85]. Children and immunosuppressed individuals are much more compromised [84,85]. During the chronic phase, an imbalance between sympathetic and parasympathetic systems involving neuronal cell destruction has been widely reported [85]. Indeed, megacolon and megaesophagus, the clinical manifestations of gastrointestinal Chagas disease, are the consequence of the autonomic nervous system dysfunction [86,87]. On the contrary, the central nervous system condition induced by *T. cruzi* infection is rare and mainly confined to immunocompromised patients [88], its symptoms are similar to those diagnosed in the acute phase but frequently more serious [85]. The underlying pathogenesis of these neurological disorders is still unknown, and is supposed to be consequence of the same pathogenic mechanisms behind the cardiac and digestive disorders: parasite persistence and self-reactive immune mechanisms developed as a result of *T. cruzi* infection [3,6,89]. Although it is not possible to rule out the presence of the parasite in different cell types of the nervous system as well as in the cerebrospinal fluid [90], antibodies against tubulin are directly associated with a broad spectrum of neurodegenerative diseases [91–94]. In particular, Kirvan et al. found that monoclonal antibodies isolated from patients with Sydenham's chorea, a central nervous system disease linked to group A streptococcal infection, reacted with a tubulin expressed in neuronal cells. The authors also questioned why the brain is the target of their monoclonal antibodies. Since tubulin is so abundant in many tissues, antibody recognition could probably be due to molecular mimicry with a bacterial extracellular lysoganglioside [92]. In the light of our findings, a longitudinal study aimed to correlate anti-tubulin sera and neurological symptoms/dysfunction in a large cohort of patients suffering different forms of Chagas disease, deems essential to understand the role of immune responses and cross-reactivity in the pathogenesis of *T. cruzi* infection.

By using phage display technology involving cDNA isolated from B cells of patients with chronic Chagas disease, we clearly demonstrate the cross-reactivity of a human antibody between *T. cruzi* and a mammal tubulin expressed only in neural tissue. The binding site of this antibody involves one of the PTMs present in trypanosomatids and this fact may probably explain the fine specific recognition of the neuronal-tubulin isotype. This work presents a conundrum: why this antibody cross-reacts only with neural tubulins?, do these tubulins have a particular PTM responsible for antibody specificity?, do anti-tubulin antibodies occur in the majority of patients with Chagas disease or only in those suffering from neurological disorders?, have these antibodies a relevant role in the outcome of pathophysiological effects?. We strongly believe that answering these questions will strengthen the significance of the auto-immune component in the context of Chagas disease not only to explain the mechanism involved in its progression but also to redefine future therapeutic strategies.

Contributors

L.L.N. and K.A.G. participated in the design of the study. L.L.N., M. P., R.G.S.C, M.S.O., V.G., M.M., D.I.S., A. P-T., G.D.A. and K.A.G. performed the experiments and statistical analysis. L.S. performed the comparative analysis of tubulin sequences. K.A.G. supervised the study. M.S.O. carried out the artwork. C.R., M.A.C. and J.M.H.R. contributed with resources. L.L.N. and K.A.G. prepared the manuscript. M.P., R.G.S.C., L.S., A.P-T., M.A.C., G.D.A. revised the manuscript. K.A.G. and M.P. reviewed and edited the final manuscript. All authors read, provided feedback and approved the final manuscript.

Declaration of Competing Interests

The authors have declared that no conflict of interest exists.

Acknowledgements

The authors are immensely grateful to sample donors involved in this study for their kind contribution. We thank to the clinical doctors from Cardiovascular Division of the Hospital General de Agudos Dr. Juan A. Fernández and Hospital General de Agudos José María Ramos Mejía, Buenos Aires, Argentina for providing human samples. Also, to Drs. Silvia Christiansen and Hernán García Rivello from the Department of Anatomical Pathology, Hospital Italiano de Buenos Aires, Buenos Aires, Argentina for the paraffin-embedded human tissue samples and Dr Rubén Laguens from Department of Pathology, Hospital Universitario Fundación Favaloro, Buenos Aires, Argentina for mouse skin slides. We also thank to Dr. Nobuko Yoshida and Dr. Sergio Schenkman from the Universidade Federal de São Paulo, Brazil for kindly providing samples of parasites and the pGEX-4T-2-alphaTub vector, Dr. Esteban Serra from Facultad de Ciencias Bioquímicas y Farmacéuticas, Universidad Nacional de Rosario, Rosario, Argentina

for generous gifts of mouse anti-α-tubulin acetylated and Dr. Esteban Bontempi from Instituto Nacional de Parasitología "Dr. Mario Fatala Chaben", Buenos Aires, Argentina for his generous donation of whole protein lysate from L. *brasiliensis*. We would also like to show our gratitude to Dr. Jon Appel for critical reading of the manuscript.

This work was envisaged by Mariano Levin, Director of the Laboratory of Molecular Biology of Chagas' disease, INGEBI-CONICET, Buenos Aires, Argentina, from 1985 to 2010. He devoted his life to untangle the pathophysiological mechanism behind this disease. He left us some time ago, but still walks with us; this manuscript is yours.

This research was supported by grants from Consejo Nacional de Investigaciones Científicas y Técnicas (CONICET; PIP No. 112-2015010-0547 to KAG) and Agencia Nacional de Promoción Científica y Tecnológica, Argentina (ANPCyT; PICT Nos. 2010-2439 and 2014-1026 to KAG and 2016-1028 to MP). The funders had no role in study design, data collection and interpretation, or the decision to submit the work for publication.

Data sharing statements

Following the National and International Code of Ethics, data relating to patients and non-infected donors privacy are not available for public access. Otherwise, the dataset generated and analyzed during the current study are available from the corresponding author on reasonable request.

Supplementary materials

Supplementary material associated with this article can be found, in the online version, at doi:10.1016/j.ebiom.2020.103206.

References

[1] World Health Organization (WHO). Fourth WHO report on neglected tropical diseases: integrating neglected tropical diseases into global health and development. IV WHO Report on Neglected Tropical Diseases; 2017.
[2] Bern C. Chagas' disease. N Engl J Med 2015;373(5):456–66.
[3] Pérez-Molina JA, Molina I. Chagas disease. Lancet 2017;391:82–94.
[4] Rassi A, Rassi A, Marin-Neto JA. Chagas disease. Lancet. 2010;375(9723):1388–402.
[5] Dutra WO, Menezes CAS, Magalhães LMD, Gollob KJ. Immunoregulatory networks in human Chagas disease. Parasite Immunol 2014;36(8):377–87.
[6] Acevedo GR, Girard MC, Gómez KA. The Unsolved Jigsaw Puzzle of the Immune Response in Chagas Disease. Front Immunol 2018;9(August):1929.
[7] Kumar S, Tarleton RL. The relative contribution of antibody production and CD8+ T cell function to immune control of Trypanosoma cruzi. Parasite Immunol 1998;20(5):207–16.
[8] Teixeira M.M., Dutra W.O., Ota M. The clinical immunology of human Chagas disease. 2005;21(12).
[9] De Bona E, Lidani KCF, Bavia L, et al. Autoimmunity in chronic chagas disease: a road of multiple pathways to cardiomyopathy? Front Immunol 2018;9(AUG):1–8.
[10] Krettli AU, Brener Z, Cançado JR. Effect of specific chemotherapy on the levels of lytic antibodies in Chagas's disease. Trans R Soc Trop Med Hyg 1982;76(3):334–40.
[11] Cordeiro FD, Martins-Filho OA, Da Costa Rocha MO, Adad SJ, Corrêa-Oliveira R, Romanha AJ. Anti-Trypanosoma cruzi immunoglobulin G1 can be a useful tool for diagnosis and prognosis of human Chagas' disease. Clin Diagn Lab Immunol 2001;8(1):112–8.
[12] Krettli AU, Weisz-Carrington P, Nussenzweig RS. Membrane-bound antibodies to bloodstream Trypanosoma cruzi in mice: strain differences in susceptibility to complement-mediated lysis. Clin Exp Immunol 1979;37(3):416–23.
[13] Krautz GM, Kissinger JC, Krettli AU. The targets of the lytic antibody response against Trypanosoma cruzi. Parasitol Today 2000;16(1):31–4.
[14] Krettli AU. The utility of anti-trypomastigote lytic antibodies for determining cure of Trypanosoma cruzi infections in treated patients: an overview and perspectives. Mem Inst Oswaldo Cruz 2009;104(SUPPL. 1):142–51.
[15] LIMA-MARTINS MVC, SANCHEZ GA, KRETTLI AU, BRENER Z. Antibody-dependent cell cytotoxicity against Trypanosoma cruzi is only mediated by protective antibodies. Parasite Immunol 1985;7(4):367–76.
[16] Martins-Filho OA, Pereira MES, Carvalho JF, Cancado JR, Brener Z. Flow cytometry, a new approach to detect anti-live trypomastigote antibodies and monitor the efficacy of specific treatment in human Chagas' disease. Clin Diagn Lab Immunol 1995;2(5):569–73.
[17] Cunha-Neto E, Teixeira PC, Fonseca SG, Bilate AM, Kalil J. Myocardial gene and protein expression profiles after autoimmune injury in Chagas' disease cardiomyopathy. Autoimmun Rev 2011;10(3):163–5.
[18] Bryan MA, Guyach SE, Norris KA. Specific humoral immunity versus polyclonal B Cell activation in trypanosoma cruzi infection of susceptible and resistant mice. PLoS Negl Trop Dis 2010;4(7).
[19] Grauert MR, Houdayer M, Hontebeyrie-Joskowciz M. Trypanosoma cruzi infection enhances polyreactive antibody response in an acute case of human Chagas' disease. Clin Exp Immunol 1993;93(1):85–92.
[20] Kerner N, Liégeard P, Levin MJ, Hontebeyrie-Joskowicz M. Trypanosoma cruzi: antibodies to a MAP-like protein in chronic chagas' disease cross-react with mammalian cytoskeleton. Exp Parasitol 1991;73(4):451–9.
[21] Petry K, Van Voorhis WC. Antigens of Trypanosoma cruzi that mimic mammalian nervous tissues: investigations of their role in the autoimmune pathophysiology of chronic Chagas' disease. Res Immunol 1991;142(2):151–6.
[22] Bonney KM, Engman DM. Autoimmune pathogenesis of chagas heart disease: looking back, looking ahead. Am J Pathol 2015;185(6):1537–47.
[23] Medei E.H., Nascimento J.H.M., Pedrosa R.C., et al. duration. 2009;10(7):868−76.
[24] Gironès N, Rodríguez CI, Basso B, et al. Antibodies to an epitope from the Cha human autoantigen are markers of Chagas' disease. Clin Diagn Lab Immunol 2001;8(6):1039–43.
[25] Borda ES, Sterin-Borda L. Antiadrenergic and muscarinic receptor antibodies in Chagas' cardiomyopathy. Int J Cardiol 1996;54(2):149–56.
[26] Gómez KA, Longhi SA, Levin MJ. The genesis of anti-cardiac G protein coupled receptor antibodies in Chagas disease. Mol Biol 2006.
[27] Ferrari I, Levin MJ, Wallukat G, et al. Molecular mimicry between the immunodominant ribosomal protein P0 of Trypanosoma crnzi and a functional epitope on the humanβ1-adrenergic receptor. J Exp Med 1995.
[28] Levy GV, Tasso LM, Longhi SA, et al. Antibodies against the Trypanosoma cruzi ribosomal P proteins induce apoptosis in HL-1 cardiac cells. Int J Parasitol 2011.
[29] Sterin-Borda L, Goin JC, Bilder CR, Iantorno G, Hernando AC, Borda E. Interaction of human chagasic IgG with human colon muscarinic acetylcholine receptor: molecular and functional evidence. Gut 2001;49(5):699–705.
[30] Beltrame SP, Auger SR, Bilder CR, Waldner CI, Goin JC. Modulation of M2 muscarinic receptor-receptor interaction by immunoglobulin G antibodies from Chagas' disease patients. Clin Exp Immunol 2011;164(2):170–9.
[31] Grippo V, Mahler E, Elias FE, et al. The heavy chain variable segment gene repertoire in chronic Chagas′ heart disease. J Immunol 2009;183(12):8015–25.
[32] Grippo V, Niborski LL, Gomez KA, Levin MJ. Human recombinant antibodies against Trypanosoma cruzi ribosomal P2β protein. Parasitology 2011;138(6):736–47.
[33] Zingales B, Miles MA, Campbell DA, et al. The revised Trypanosoma cruzi subspecific nomenclature: rationale, epidemiological relevance and research applications. Vol. 12. Infect Genet Evol 2012:240–53.
[34] Teixeira MMG, Yoshida N. Stage-specific surface antigens of metacyclic trypomastigotes of Trypanosoma cruzi identified by monoclonal antibodies. Mol Biochem Parasitol 1986;18(3):271–82.
[35] Wirtz E, Leal S, Ochatt C, Cross GAM. A tightly regulated inducible expression system for conditional gene knock-outs and dominant-negative genetics in Trypanosoma brucei. Mol Biochem Parasitol 1999;99(1):89–101.
[36] Guo J, Walss-Bass C, Ludueña RF. The β isotypes of tubulin in neuronal differentiation. Cytoskeleton 2010.
[37] Finnern R, Pedrollo E, Fisch I, et al. Human autoimmune anti-proteinase 3 scFv from a phage display library. Clin Exp Immunol 1997;107(2):269–81.
[38] Hoet RMA, Pieffers M, Stassen MHW, et al. The importance of the light chain for the epitope specificity of human anti-U1 small nuclear RNA autoantibodies present in systemic lupus erythematosus patients. J Immunol 1999;163(6):3304–12.
[39] G.S. Chirivi R. Anti-citrullinated protein antibodies as novel therapeutic drugs in rheumatoid arthritis. J Clin Cell Immunol 2013;01(S6):1–13.
[40] Breitling R, Klingner S, Callewaert N, et al. Non-pathogenic trypanosomatid protozoa as a platform for protein research and production. Protein Expr Purif 2002.
[41] Ferrer MJ, Wehrendt DP, Bonilla M, Comini MA, Tellez-Iñón MT, Potenza M. Production of recombinant trypanosoma cruzi antigens in leishmania tarentolae. Methods Mol Biol 2019;1955:105–18.
[42] Longhi SA, Atienza A, Perez Prados G, et al. Cytokine production but lack of proliferation in peripheral blood mononuclear cells from chronic Chagas' disease cardiomyopathy patients in response to T. cruzi ribosomal P proteins. PLoS Negl Trop Dis 2014.
[43] Wilm M, Shevchenko A, Houthaeve T, et al. Femtomole sequencing of proteins from polyacrylamide gels by nano-electrospray mass spectrometry Vol. 379 Nature 1996:466–9.
[44] The UniProt Consortium. UniProt: a worldwide hub of protein knowledge The UniProt Consortium. Nucleic Acids Res. 2019.
[45] Aslett M, Aurrecoechea C, Berriman M, et al. TriTrypDB: a functional genomic resource for the Trypanosomatidae. Nucleic Acids Res 2009.
[46] Görg A, Obermaier C, Boguth G, et al. The current state of two-dimensional electrophoresis with immobilized pH gradients. Electrophoresis 2000;21(6):1037–53.
[47] Bonhivers M, Landrein N, Decossas M, Robinson DR. A monoclonal antibody marker for the exclusion-zone filaments of Trypanosoma brucei. Parasites Vectors 2008;1(1):1–8.
[48] Sievers F, Wilm A, Dineen D, et al. Fast, scalable generation of high-quality protein multiple sequence alignments using Clustal omega. Mol Syst Biol 2011;7(539).
[49] Stothard P. The sequence manipulation suite: javaScript programs for analyzing and formatting protein and DNA sequences. BioTechniques 2000.
[50] Wu L, Oficjalska K, Lambert M, et al. Fundamental characteristics of the immunoglobulin V H repertoire of chickens in comparison with those of humans, mice, and camelids. J Immunol 2012;188(1):322–33.
[51] Cain JA, Solis N, Cordwell SJ. Beyond gene expression: the impact of protein post-translational modifications in bacteria. J Proteomics 2014;97:265–86.

[52] Sinclair AN, de Graffenried CL. More than microtubules: the structure and function of the subpellicular array in trypanosomatids. Trends Parasitol 2019;35(10):760–77.
[53] Hammers, Christoph M, Stanley JR. Antibody phage display: technique and applications Christoph. J Invest Dermatol 2014;134(2):1–13.
[54] Little M, Seehaus T. Comparative analysis of tubulin sequences. Comp Biochem Physiol - Part B 1988.
[55] Banerjee A, Jensen-Smith H, Lazzell A, et al. Localization of βV tubulin in the cochlea and cultured cells with a novel monoclonal antibody. Cell Motil Cytoskeleton 2008;65(6):505–14.
[56] Gadadhar S, Bodakuntla S, Natarajan K, Janke C. The tubulin code at a glance. J Cell Sci 2017.
[57] Schneider A, Plessmann U, Weber K. Subpellicular and flagellar microtubules of Trypanosoma brucei are extensively glutamylated. J Cell Sci 1997;110(4):431–7.
[58] Nogales E, Wolf SG, Zhang SX, Downing KH. Preservation of 2-D crystals of tubulin for electron crystallography. J Struct Biol 1995;115:199–208.
[59] Nogales E, Wolf SG, Downing KH. Structure of the αβ tubulin dimer by electron crystallography. Nature 1998;391(6663):199–203.
[60] Löwe J, Li H, Downing KH, Nogales E. Refined structure of αβ-tubulin at 3.5Å resolution. J Mol Biol 2001;313(5):1045–57.
[61] Ludueña RF. Are tubulin isotypes functionally significant. Mol Biol Cell 1993;4(5):445–57.
[62] Ludueña RF. Multiple forms of tubulin: different gene products and covalent modifications. Int Rev Cytol 1997;178:207–75.
[63] Lu Q, Moore GD, Walss C, Ludueña RF. Structural and functional properties of tubulin isotypes. Adv Struct Biol 1999;5(C):203–27.
[64] Song Y, Brady ST. Post-translational modifications of tubulin: pathways to functional diversity of microtubules. Trends Cell Biol 2015;25(3):125–36.
[65] Wloga D, Joachimiak E, Fabczak H. Tubulin post-translational modifications and microtubule dynamics. Int J Mol Sci 2017;18(10).
[66] Nogales E. Structural insights into microtubule function. Annu Rev Biochem 2000.
[67] Gull K. The cytoskeleton of trypanosomatid parasites. Annu Rev Microbiol 1999.
[68] Alcina A, Hargreaves AJ, Avila J, Fresno M. A Trypanosoma cruzi monoclonal antibody that recognizes a superficial tubulin-like antigen. Biochem Biophys Res Commun 1986.
[69] Alcina A, Hargreaves AJ, Avila J, Hesketh JE, Fresno M. The detection of a spectrin-like protein in Trypanosoma cruzi with a polyclonal antibody. Cell Biol Int Rep 1988;12(11):979–85.
[70] Ternynck T, Bleux C, Gregoire J, Avrameas S, Kanellopoulos-Langevin C. Comparison between autoantibodies arising during Trypanosoma cruzi infection in mice and natural autoantibodies. J Immunol 1990.
[71] Kahn S, Kahn M, Eisen H. Polyreactive autoantibodies to negatively charged epitopes following Trypanosoma cruzi infection. Eur J Immunol 1992;22(12):3051–6.
[72] Montalvão F, Nascimento DO, Nunes MP, et al. Antibody repertoires identify β-tubulin as a host protective parasite antigen in mice infected with Trypanosoma cruzi. Front Immunol 2018;9(APR):1–9.
[73] Ribeiro Dos Santos R, Marquez JO, von Gal Furtado CC, Ramos de Oliveira JC, Martins AR, Köberle F. Antibodies against neurons in chronic Chagas' disease. Tropenmed Parasitol 1979.
[74] Gea S, Ordonez P, Cerban F, Iosa D, Chizzolini C, Vottero-Cima E. Chagas' disease cardioneuropathy: association of anti-Trypanosoma cruzi and anti-sciatic nerve antibodies. Am J Trop Med Hyg 1993.
[75] MINOPRIO P, BURLEN O, PEREIRA P, et al. Most B cells in acute Trypanosoma cruzi infection lack parasite specificity. Scand J Immunol 1988.
[76] Ortiz-Ortiz L, Parks DE, Rodriguez M, Weigle WO. Polyclonal B lymphocyte activation during Trypanosoma cruzi infection. J Immunol 1980;124(1):121–6.
[77] Rojas M, Restrepo-Jiménez P, Monsalve DM, et al. Molecular mimicry and autoimmunity. J Autoimmun 2018;95(September):100–23.
[78] Bao W, Yuan CA, Zhang Y, et al. Mutli-features prediction of protein translational modification sites. IEEE/ACM Trans Comput Biol Bioinforma 2018;15(5):1453–60.
[79] Gianazza E, Parravicini C, Primi R, Miller I, Eberini I. In silico prediction and characterization of protein post-translational modifications. J Proteomics 2016;134:65–75.
[80] Janke C, Kneussel M. Tubulin post-translational modifications: encoding functions on the neuronal microtubule cytoskeleton. Trends Neurosci 2010;33(8):362–72.
[81] Mattos EC, Schumacher RI, Colli W, Alves MJM. Adhesion of trypanosoma cruzi trypomastigotes to fibronectin or laminin modifies tubulin and paraflagellar rod protein phosphorylation. PLoS ONE 2012;7(10).
[82] Fukushima N, Furuta D, Hidaka Y, Moriyama R, Tsujiuchi T. Post-translational modifications of tubulin in the nervous system. J Neurochem 2009;109(3):683–93.
[83] Zhang F, Su B, Wang C, et al. Posttranslational modifications of α-tubulin in alzheimer disease. Transl Neurodegener 2015.
[84] Pittella JE. Central nervous system involvement in Chagas' disease. An updating. Rev Inst Med Trop São Paulo 1993;35:111–6.
[85] Py MO. Neurologic manifestations of chagas disease. Curr Neurol Neurosci Rep 2011;11(6):536–42.
[86] Matsuda NM, Miller SM, Evora PRB. The chronic gastrointestinal manifestations of Chagas disease. Clinics 2009;64(12):1219–24.
[87] de Oliveira ÊC, da Silveira ABM, Luquetti AO. Gastrointestinal Chagas disease. Birkhauser Adv Infect Dis 2019:243–64.
[88] Chimelli L., Scaravilli F. Trypanosomiasis. Brain pathology. 1997.
[89] Teixeira ARL, Hecht MM, Guimaro MC, Sousa AO, Nitz N. Pathogenesis of chagas' disease: parasite persistence and autoimmunity. Clin Microbiol Rev 2011;24(3):592–630.
[90] Córdova E, Maiolo E, Corti M, Orduña T. Neurological manifestations of Chagas' disease. Neurol Res 2010;32(3):238–44.
[91] Connolly AM, Pestronk A, Trotter JL, Feldman EL, Cornblath DR, Olney RK. High−titer selective serum anti−β−tubulin antibodies in chronic inflammatory demyelinating polyneuropathy. Neurology 1993.
[92] Kirvan CA, Cox CJ, Swedo SE, Cunningham MW. Tubulin is a neuronal target of autoantibodies in sydenham's chorea. J Immunol 2007;178(11):7412–21.
[93] Švarcová J, Fialová L, Bartoš A, Šteinbachová M, Malbohan I. Cerebrospinal fluid antibodies to tubulin are elevated in the patients with multiple sclerosis. Eur J Neurol 2008;15(11):1173–9.
[94] Abou-Donia MB, Lieberman A, Curtis L. Neural autoantibodies in patients with neurological symptoms and histories of chemical/mold exposures. Toxicol Ind Health 2018;34(1):44–53.